Spatial Coding in the Subiculum Requires Anterior Thalamic Inputs

Bethany E. Frost[1], Matheus Cafalchio[1], Sean K. Martin[1], Md Nurul Islam[1], John P. Aggleton[2], Shane M. O'Mara[1*]

[1]Institute of Neuroscience, Trinity College Dublin, Dublin, Ireland; [2]School of Psychology, Cardiff University, Cardiff, United Kingdom

*For correspondence: smomara@tcd.ie

Summary

Hippocampal function relies on the anterior thalamic nuclei, yet the reasons remain poorly understood. While anterior thalamic lesions disrupt parahippocampal spatial signalling, their impact on the subiculum is unknown, despite the importance of this area for hippocampal networks. We recorded subiculum cells in rats with either permanent (*N*-methyl-D-aspartic acid) or reversible (muscimol) anterior thalamic lesions. The diverse spatial signals normally found in the subiculum, including place cells, disappeared following permanent thalamic lesions and showed marked disruption during transient lesions. Meanwhile, permanent anterior thalamic lesions had no discernible impact on CA1 place fields. Thalamic lesions reduced spatial alternation performance (permanently or reversibly) to chance levels, while leaving a non-spatial recognition memory task unaffected. These findings, which help to explain why anterior thalamic damage is so deleterious for spatial memory, cast a new spotlight on the importance of subiculum function, and reveal its dependence on anterior thalamic signalling.

Keywords: Electrophysiology, Hippocampus, Navigation, Space, Anterior Thalamus, Reversible Lesion, Spatial cells, Subiculum

Introduction

The hippocampal formation lies at the heart of the brain's cognitive mapping capabilities, while also comprising part of an extended system vital for human episodic memory (Spiers et al., 2001; Ranganath and Ritchey, 2012; O'Mara and Aggleton, 2019). The anterior thalamic nuclei (ATN) are key structures within both functional systems (Aggleton and Brown, 1999; Ranganath and Ritchey, 2012). In rodents, for instance, anterior thalamic lesions severely impair spatial learning, echoing the effects of hippocampal damage (Morris et al., 1982; Sutherland and Rodriguez, 1989; Warburton and Aggleton, 1999; Moran and Dalrymple-Alford, 2003), with disconnection studies confirming the interdependence of the hippocampal formation and anterior thalamus (Warburton et al., 2000, 2001; Henry et al., 2004). Moreover, neuronal recordings within the ATN show the presence of place, head direction and border cells (Taube, 1995; Jankowski et al., 2015; Matulewicz et al., 2019), suggesting the ATN is also a spatial processing node. Outstanding questions include whether any hippocampal formation spatial functions are dependent on the ATN and, if so, why.

Attention focussed on the subiculum, the principal hippocampal recipient of direct projections from the anteroventral and anteromedial thalamic nuclei (Shibata, 1993; O'Mara et al., 2001). The subiculum contains cells with a variety of spatial properties, including place and grid cells, as well as boundary vector cells (Anderson and O'Mara, 2004; Lever et al., 2009; Brotons-Mas et al., 2010; 2017). The relationship of these subiculum cell-types to the ATN remains unknown, though it might readily

be assumed that the dense inputs from area CA1, with its numerous 'place' cells (O'Keefe, 1979; Moser et al., 2008) are sufficient for effective subiculum place cells. Likewise, inputs from entorhinal cortex (Moser et al., 2008) could potentially ensure subiculum grid cells. Here, we questioned these assumptions by determining whether the spatial properties of subiculum cells depend on ATN activity.

The importance of the ATN for parahippocampal activity has, by comparison, received far more attention. Anterior thalamic lesions involving the anterodorsal nucleus eliminate parahippocampal head-direction signals (Goodridge and Taube, 1997; Winter et al., 2015), while reducing the periodicity and frequency of parahippocampal grid cell activity (Winter et al., 2015). Nevertheless, disruption of the head-direction network does not explain the severity or diversity of the spatial learning deficits following ATN lesions (Vann and Aggleton, 2004; Aggleton, 2005; Dudchenko et al., 2005; Dillingham and Vann, 2019). Head-direction system lesions (including the lateral mammillary nucleus, which provides head-direction signals for the ATN; Sharp and Koester, 2008), cause appreciably milder spatial deficits than ATN lesions (Aggleton et al., 1991; 1995; Vann, 2005, 2018; Perry et al., 2018). The conclusion is that the ATN contribute in additional ways to spatial processing.

Following our evidence that ATN lesions largely abolish subiculum spatial signalling and reduce spatial alternation performance to chance, we next tested the anatomical specificity of this disconnection effect by recording hippocampal CA1 place cells after ATN lesions. The very dense CA1 projections to the subiculum (Amaral et al., 1991; Cembrowski et al., 2018; van Strien et al., 2009), which potentially supply the subiculum with spatial information (O'Mara, 2005), provide the rationale for determining the sensitivity of CA1 to ATN damage (see Calton et al., 2003). The key question was whether the impact on the subiculum in the first experiment reflected upstream changes in CA1. We found that, although spatial alternation performance was at chance, place cell discharge in CA1 appeared unaffected.

Results

Throughout, the terms hippocampal formation and hippocampal refer to the dentate gyrus, the CA fields, and the subiculum (Burwell & Witter, 2002). The parahippocampal region includes the presubiculum, parasubiculum, postsubiculum and entorhinal cortices.

Effect of anterior thalamic lesions on spatial processing in dorsal subiculum

Of 20 animals implanted, one rat with an anterior thalamic lesion (ATNx) was subsequently excluded due to electrode malfunction while one normal control experienced post-surgical complications and was also excluded. Comparisons between the two control groups consistently failed to reveal group differences and for this reason they were typically combined (group 'CControl').

Lesion analysis: Permanent (N-methyl-D-aspartic acid) anterior thalamic lesions

Lesion size was quantified by comparing anti-NeuN reacted cell counts in the anteromedial, anterodorsal, and anteroventral thalamic nuclei in lesioned animals to CControl values (Fig. 1A, B). The ATNx rats had markedly reduced cell counts (CControl 16209 ± 2507, ATNx 3497 ± 1528; t = -9.68, df = 8.26, $p < 0.001$, Welch's Two Sample *t*-test; Fig. 1E), while the calbindin-reacted sections indicated that nucleus reuniens remained intact (Fig. 1C, D), i.e., was not a contributing factor.

Behaviour

Unless otherwise stated, Welch's Two Sample *t*-tests were performed to compare CControl and lesion data.

During free exploration in the square arenas with electrophysiological recordings, the ATNx rats travelled greater distances than the CControl animals during habituation (CControl 62.14 ± 17.43, ATNx 85.45 ± 14.21; t = 3.55, df = 16.14, p = 0.0026) and during subsequent recordings (CControl 120.66 ± 15.19, ATNx 142.41 ± 10.89; t = 2.98, df = 14.55, p = 0.0096), suggesting heightened motor activity.

Consistent with previous lesion studies, ATNx animals had considerably lower spatial alternation scores (52.23 ± 14.58%), compared to Normal (83.10 ± 10.96%) and Sham (81.25 ± 11.41%) controls (ANOVA $p < 0.001$, Tukey post-hoc $p < 0.001$; Fig. 2B), confirming their severely impaired spatial working memory.

In contrast, ATNx animals showed no impairment in novel object discrimination when compared to the CControl animals ($p > 0.05$), indicating that recognition memory under these conditions remains intact (Fig 2D-F).

Single unit activity: Subiculum

Spatial and non-spatial single units were recorded in the dorsal subiculum of all animals. Of 72 single units recorded in the CControl rats, 55 (76%) were considered spatial units. These units consisted of place (n = 19; 21%), head direction (n = 19; 21%), place x head direction (n = 3; 3%), border (n = 6; 7%) and grid (n = 8; 9%) cells. A further 17 (24%) did not show obvious spatial properties. Strikingly, no spatial units were recorded in the ATNx animals, although non-spatial units (16) were present.

Of the 55 spatial units recorded in the CControl animals, place-, grid- and head direction cells remapped in response to rotated visual cues.

Spike properties

The mean spike width of all subicular cells grouped was greater in ATNx animals than CControls in regular spiking (CControl 149.41 ± 40.78, ATNx 220.57 ± 63.95; t = 2.71, df = 9.58, p = 0.023) and bursting cells (CControl 142.14 ± 43.87, ATNx 200.63 ± 41.15; t = 4.46, df = 17.60, $p < 0.001$). Other spike properties (top section, Table 1), including number of spikes, spike frequency, amplitude, height, and inter-spike interval, showed no differences between groups ($p > 0.05$).

When non-spatial cells in CControl animals were compared to putative 'non-spatial' cells in ATNx animals, both spike height and spike width were greater in animals that had ATN lesions (spike height CControl 129.63 ± 38.45, ATNx 157.11 ± 38.21; t = 2.78, df = 50.78, p = 0.0076, Fig. 4J; spike width CControl 168.63 ± 57.78, ATNx 208.37 ± 51.43; t = 2.86, df = 55.14, p = 0.0061, Fig. 4K).

Bursting cells

As no spatial units were recorded in ATNx animals, it was unclear whether spatial cells were present but inhibited (and, therefore, not recorded) or whether the units that were recorded were latent spatial units that were now not responding to 'spatial' inputs. Due to the difficulties in comparing non-spatial units in the CControls to unknown spatial or non-spatial units in ATNx animals, subicular cells were classified according to their spike properties into bursting, fast spiking, and theta-entrained cells (Anderson and O'Mara, 2003).

While the percentage of subiculum bursting cells in the CControl (56% of 72 units) and ATNx (52% of 16) animals was essentially equivalent, other properties differed (lower section Table 1, Fig. 4). Cells

in CControl animals showed a greater propensity to burst than those in lesion animals (CControl 0.1 ± 0.08, ATNx 0.05 ± 0.05; t = 3.76, df = 48.68, p < 0.001; Table 1). Bursting cells in CControl animals showed more spikes per burst (CControl 2.15 ± 0.14, ATNx 2.08 ± 0.12; t = 2.09, df = 33.01, p = 0.044) and greater burst duration (CControl 5.71 ± 0.75, ATNx 5.22 ± 0.76; t = 2.66, df = 28.29, p = 0.013), and conversely lesion animals showed larger inter-burst intervals than controls (CControl 28074 ± 44912, ATNx 78167 ± 99288; t = -2.21, df = 21.68, p = 0.038; Table 1).

Lesion Analysis: Reversible (muscimol) anterior thalamic lesions

Behaviour

When the ATN was temporarily inactivated with muscimol, spatial alternation dropped to chance levels (Fig. 5B). Two animals also received bilateral saline infusions as a control, showing no deficit in spatial alternation.

Single unit activity: Subiculum

Prior to the muscimol infusion sessions, electrophysiological recordings were conducted on cannulated rats to allow for electrode adjustment and habituation to recording equipment. Single units were recorded during these habituation periods, however, only units recorded during the inactivation experiments were considered. Thirty-five cells were recorded during muscimol experiments. Of these, 29 were recorded at baseline, i.e., immediately prior to muscimol infusion, and used for analysis.

Spike properties

For analysis, unless otherwise stated, Welch's Two Sample *t*-tests were again performed to consider cell parameters with respect to baseline data. When all cells were grouped together, mean spiking frequency decreased immediately following ATN inactivation (Fig. 6A), although the number of spikes per recording session decreased in the first 20 minutes (p < 0.001, Fig. 6B) then returned to baseline the following day. Mean spike amplitude increased after inactivation (Fig. 6C) returning to baseline the following day. There was an increase in mean spike height after ATN inactivation before returning to baseline (Fig. 6D), whereas mean spike width remained at baseline for several hours following muscimol infusion (Fig. 6E). Finally, when all units were grouped, temporary inactivation of ATN led to an increase in inter spike interval (ISI) before returning to baseline the following day (Fig. 6F).

Spatial properties

Of the 29 cells recorded at baseline, 17 were considered non-spatial and 12 spatial immediately prior to muscimol infusion. These spatial units consisted of head direction (2), place (3), border (2) and grid (5) cells.

Following muscimol infusion, spatial properties of these cells was observed to decline, despite no decrease in firing frequency. For designated place cells prior to infusion, the place field became disrupted after ATN inactivation (Fig. 5A1). Head directionality became disrupted without ATN input (Fig. 5A2) and grid cells did not fire in a grid-like pattern (Fig. 5A3). In the majority of cases, these spatial properties were recovered by the following day, although in some cases the cells were no longer recorded (Fig. 5C3). Interestingly, the grid cells appeared to lose their place field initially but retained some head directionality, before this too was disrupted (Fig 5A3, 5C1-2).

Burst properties

Of the 29 units included in the study, at baseline 20 were classified as bursting, 6 fast spiking, and 2 theta modulated (prior to muscimol infusion). For spike property analysis, theta modulated units were excluded due to the high firing frequency and insufficient numbers to perform further statistical analysis.

When fast spiking and bursting units were combined, there was no difference in firing frequency compared to baseline, following ATN inactivation with muscimol (Fig. 6A). All animals travelled less distance, i.e. showed less activity, throughout the experiment (as time increased; Fig. 6B), although there was no correlation between firing frequency and distance travelled (Fig. 6C).

Bursting units did not show any changes in burst properties following inactivation of the ATN, including number of spikes, spikes per burst, and burst duration ($p > 0.05$). Cells that had been specified spatial units prior to infusion showed no changes in burst properties or firing frequency, indicating that these spatial cells continue to fire following ATN inactivation but no longer displayed spatial properties.

Effect of anterior thalamic lesions on spatial processing in CA1

In order to explore the effect of anterior thalamic lesion on spatial processing in the dorsal hippocampus, a further 3 rats were implanted with a microdrive apparatus with 8 tetrodes into the dorsal CA1 and received bilateral (N-methyl-D-aspartic acid) lesions in the anterior thalamus. As in the previous experiment, lesions were quantified by comparing anti-NeuN reacted cell counts in the anterior thalamic nuclei to CControl cell counts. In all ATNx_CA1 animals the surgery consistently produced marked cell loss throughout almost the entire anterior thalamus. An independent sample *t*-test showed significant difference in anti-NeuN cell counts between ATNx_CA1 (4166 ± 1003) and CControl ($p < 0.001$, $t = 9.08$, $df = 7$, Welch's Two Sample *t*-test).

Lesion analysis: Hippocampal area CA1, post- permanent anterior thalamic lesions

Behaviour

As expected, ATNx_CA1 rats showed a deficit in spatial alternation on the T-maze, equivalent to ATNx animals (ATNx_CA1 52.60 ± 11.40%, $t = -10.71$, $df = 40.93$, $p < 0.001$; Fig. 7C), confirming an impairment in spatial working memory. These animals also showed no deficit in object recognition and no difference in overall exploration time, compared to CControl ($p > 0.05$; Fig.7D1-3).

Single unit activity: CA1

ATNx_CA1 animals were recorded daily performing a pellet-chasing task in an open field. From these animals 203 well isolated units were recorded from dorsal CA1. Units were further classified into 107 spatial units using sparsity and coherence criteria (rat 1 n=12; rat 2 n=67; rat 3 n=28) (Schoenenberger et al., 2016). Despite the absence of spatial signal in the subiculum, hippocampal place cells appeared intact (Fig 7E).

Discussion

We examined the role of the anterior thalamic nuclei in the extended hippocampal formation, by combining *in vivo* neurophysiological recordings, permanent and reversible lesions, and behavioural analyses. As expected, in control animals, i.e., with an intact ATN, there is normal spatial firing in hippocampal area CA1 (place cells) and subiculum (place, head direction, grid and border cells). After

ATN lesions, CA1 place activity appeared preserved, whereas the usual heterogeneous subicular spatial activity was lost. Moreover, post-ATN lesion performance was at chance for spatial alternation but intact for the object recognition memory task, indicating a specific rather than generalised deficit. These same effects were reversible when using a transient or temporary lesion: consequently, spatial firing and spatial alternation performance were reinstated after the temporary inactivation of the ATN.

More restricted lesions centred on the anterodorsal nucleus, disrupt the head direction signal but leave CA1 place cells largely intact, despite some loss of coherence and information content (Calton et al., 2003). Meanwhile, our complete ATN lesions left CA1 place cells intact. Given that the majority of pyramidal cells in CA1 are place cells and that CA1 heavily innervates the subiculum, it could be assumed that many subiculum spatial cells are principally driven by their CA1 inputs. This latter view now seems untenable, because contrary to that prediction, projections from ATN instead appear crucial for supporting subicular spatial cellular discharge, alongside (behavioural) spatial alternation. These results not only reaffirm the view that the ATN have a significant role to play in navigation, but also reveal that the significance of the subiculum might be much greater than often thought, given the severity of the behavioural deficit despite the sparing of CA1 spatial properties. As the subiculum is the principal source of hippocampal projections beyond the temporal lobe, these findings also reveal how anterior thalamic damage might indirectly impact upon a wide array of other sites, including the mammillary bodies and retrosplenial cortex (RSC) (Ferguson et al., 2019; Haugland et al., 2019).

Consistent with previous reports, we found spatial cells, including grid-like cells, in the dorsal subiculum of healthy, control animals; however, no spatial units were recorded in the dorsal subiculum of ATN-lesioned animals. Within-animal trials were used to confirm this phenomenon, whereby the ATN was temporarily inactivated using micro-infusions of muscimol. Spatial activity was lost as muscimol took effect, and recovered as muscimol was metabolised. These effects, which presumably arise from the loss of AM and AV discharge to the subiculum, alongside AD disconnection from the pre-, post-and parasubiculum, show the closeness of this relationship.

Although grid cells (Hafting et al., 2005) have been widely studied in the hippocampal formation since their discovery in the medial entorhinal cortex (mEC) and pre/post subiculum, the disclosure here of grid cells in the dorsal subiculum is still relatively new (Brotons-Mas et al., 2017). Grid cells had, however, been previously reported in the pre- and parasubiculum (Boccara et al., 2010); parahippocampal areas that receive inputs from the anterior thalamic nuclei (van Groen and Wyss, 1990). The grid-like signal found in these regions could, therefore, be thalamic rather than entorhinal in origin. In addition to the head-direction cells in the anterodorsal thalamic nucleus, the anteroventral nucleus possesses theta-modulated head-direction cells (Tsanov et al., 2011), while the anteromedial nucleus contains place cells and perimeter/boundary cells (Jankowski et al., 2015; Matulewicz et al., 2019). Bonnavie et al. (2013) demonstrated that when the hippocampus was inactivated with muscimol, entorhinal grid cells lost their periodicity resulting in head direction cells. Here, when the ATN was inactivated with muscimol, place fields of subicular grid cells became disrupted and head directionality seemingly became more prominent.

Stewart and Wong (1993) originally observed *in vitro* that subicular cells can be classified into bursting and non-bursting classes; subsequently, Sharp and Greene (1994) confirmed this classification *in vivo.* Anderson and O'Mara (2003), in a fuller *in vivo* analysis, concluded that subicular units could be separated into bursting, regular spiking, theta-modulated, and fast spiking units. Here, we found that although the proportions of bursting cells seem unchanged, their properties were altered after anterior thalamic lesions. The proportion of bursting cells in the CControl and ATNx were

equivalent, but some of their other phenotypic properties differed: controls showed a greater propensity to burst, as well as having more spikes per burst and greater burst duration. Conversely, lesion animals showed larger inter-burst intervals than controls. This alteration in bursting may affect the fidelity of subicular-retrosplenial transmission (Nitzan et al., 2019).

The ATN lesion effects matched those of hippocampal lesions: severely impaired T-maze alternation, but spared object recognition in the bow-tie maze (Albasser et al., 2012). We found increased motor activity in ATNx rats in square arenas, but an inconsistent decrease in overall object exploration in the recognition task. The former matches prior evidence of activity increases following ATN lesions in spatial settings (e.g., Dumont & Aggleton, 2013; Poirier & Aggleton, 2009; Warburton et al., 1999) potentially linked to a failure to encode and retain locations, a finding also seen after hippocampal damage (e.g., Gray & McNaughton, 1983; Davidson & Jarrard, 2004).

The consensus has been that the subiculum is the primary output of the hippocampal formation area CA1 (Amaral et al., 1991; Cembrowski et al., 2019), with its substantial preponderance of place cells, ensuring the input to subiculum is principally spatial in nature. Our data suggest another surprising possibility: there are (at least two) parallel spatial processing networks: one, a 'hippocampus proper' pathway (centred on EC-DG-CA3-CA1-EC), and a second one beginning with ATN-SUB connections, which then interact directly with frontal and retrosplenial cortices. Both networks receive substantial entorhinal inputs. These two networks presumably interact, e.g., in the subiculum, helping to explain the severity of the ATN lesion effects. This analysis also suggests that the very substantial input from CA1 to the subiculum supports some other aspect of behavioural performance. One possibility is that it supports non-spatial aspects of memory, e.g., temporal bridging (Hampson and Deadwyler, 2004).

Overall, the data presented here show that ATN inputs to the subiculum centrally support spatial activity in the subiculum, contributing to spatial alternation performance. Further, these data indicate that signalling within the rest of the hippocampus (e.g., CA1) is not sufficient for the varied spatial signals found in the subiculum. We suggest that spatial signals found in subiculum arise from converging inputs from the various anterior thalamic nuclei, augmented by parahippocampal inputs, e.g., from entorhinal cortex. Further work is required to determine the nature of the computations performed by subiculum on the inputs it receives from ATN; how transformation rules are applied to these inputs to support spatial alternation performance; and to discover the functions of the substantial input from hippocampal area CA1, which may either prove to be substantially non-spatial in nature or be critically gated by convergent ATN projections to the subiculum.

Materials and Methods

Subjects

Experiments were conducted on 23 male Lister Hooded rats (Envigo, UK) with pre-procedural weights of 309-356g. Upon arrival, animals were cohoused on a 12-hour day/night cycle and handled daily by the experimenter for a week before surgical procedure. Prior to surgery and during recovery, animals had free access to food and water; during behavioural testing, food was restricted to within 85% of the animal's free feeding weight. All rats were naïve prior to the present study. Selection of animals between lesion and control groups was alternated according to body weight prior to surgery (starting with the heaviest), so that pre-procedural weights were matched and the groups balanced.

During stereotaxic surgery, rats were implanted unilaterally with twenty-eight electrodes of 25µm thickness platinum-iridium wires (California FineWire, USA) arranged in a tetrode formation. Tetrodes

were targeted at the dorsal subiculum, CA1, or at the subiculum and CA1 simultaneously. An additional bipolar electrode (stainless steel, 70µm thickness) targeting the ipsilateral retrosplenial cortex (RSP) was also implanted in all but two cases (see below), the data from which are considered elsewhere. All electrodes were connected to a 32-channel microdrive (Axona Ltd., UK).

For the permanent lesion experiments ten animals received stereotaxic cytotoxic lesions targeting the anterior thalamic nuclei ('ATNx'), followed by electrode implantation. Of these ten, seven had electrodes targeting dorsal subiculum and three had electrodes targeting CA1. Meanwhile three rats underwent sham injections of equivalent volumes of PBS only ('Sham' controls). A further four rats ('Normal' controls) had no sham lesion procedure, i.e., just had electrodes implanted. Both the sham and normal controls had electrodes targeting dorsal subiculum.

The temporary inactivation (muscimol) experiment, followed the permanent lesion study. For this, a further six animals (ATNmusc) were implanted with tetrode and bipolar electrode configurations alongside bilateral infusion cannulae (26 gauge, 4mm length, Bilaney Consultants Ltd., UK) in the ATN. Electrodes were positioned as above, with two exceptions; one animal was implanted with four tetrodes targeting the subiculum, three targeting CA1 and one targeting retrosplenial cortex, with no additional bipolar electrode; and one rat was implanted with tetrodes targeting the subiculum and the bipolar electrode targeting CA1.

Ethics

All experimental procedures were in accordance with the ethical, welfare, legal and other requirements of the Healthy Products Regulatory Authority regulations, and were compliant with the Health Products Regulatory Authority (Irish Medicines Board Acts, 1995 and 2006) and European Union directives on Animal Experimentation (86/609/EEC and Part 8 of the EU Regulations 2012, SI 543). All experimental procedures were approved by the Comparative Medicine/Bioresources Ethics Committee, Trinity College Dublin, Ireland prior to conduct, and were carried out in accordance with LAST Ireland and international guidelines of good practice.

Surgical methods - permanent ATN lesions and electrode placements

Detailed descriptions of surgical methods can be found elsewhere (Jankowski et al., 2014). Briefly, rats were anaesthetised with isoflurane (5% to induce anaesthesia, 1-2% to maintain) combined with oxygen (2 L/minute). After being placed in a stereotaxic frame, chloramphenicol 0.5% eye gel, pre-operative antibiotics (Enrocare, 0.1ml in 0.5ml saline) and analgesia (Metacam, 0.1ml) were administered.

The skull was exposed and connective tissue sectioned. For the ATNx cohort (n = 7), bilateral neurotoxic lesions targeting the ATN were performed using slow infusions of 0.12M *N*-methyl-D-aspartic acid (NMDA) dissolved in phosphate buffer solution (PBS, pH 7.35). NMDA was infused over 5 minutes (0.22 or 0.24µl per site) via a 0.5µl Hamilton syringe (25 gauge), with the syringe left in position a further 5 minutes at each of four target sites before slow retraction. The craniotomies were sealed using bone wax (SMI, St Vith, Belgium). The ATN lesion coordinates, with the skull flat, were as follows from bregma: AP -1.7mm, ML ±0.8mm, DV -5.7mm from top of cortex; AP -1.7mm, ML ±1.6mm, DV -4.9mm from top of cortex. Sham control animals (n=3 rats) underwent four equivalent infusions of PBS only.

Tetrodes were implanted aimed at the dorsal subiculum (AP -5.6mm, ML 2.5mm, DV -2.7mm from top of cortex) or at both the subiculum and CA1 (AP -3.8mm, ML 2.5 mm, DV -1.40mm from top of cortex).

Electrodes were stabilised with dental cement (Simplex Rapid, Kemdent, UK) attached to screws implanted into the skull.

Glucosaline was administered subcutaneously post-operatively and the animal allowed to recover. Animal weight, activity, and hydration were closely monitored daily for a minimum of 7 days before beginning electrophysiological recordings.

Electrophysiological recordings

Electrophysiological recordings were obtained using an Axona Ltd (UK) 64-channel system, allowing dual recordings of single units and local field potentials (LFP) from each electrode. Initial habituation recordings were conducted in a 60 x 60 cm square, walled arena (height 42 cm). Later testing involved a larger arena (105 x 105 cm, 25 cm height). For both arenas the walls and floors were made of wood painted matt black. A black curtain could be closed around the arena to remove distal spatial cues, and visual cues could be attached to the curtain as required. The habituation sessions in the small arena allowed the animal to acclimatise to the recording procedure and the experimenter to adjust electrode locations until the optimal recording depth was reached. After the habituation period (usually 3-7 days), rats were first trained on the behavioural tasks (T-maze then bow-tie maze) with up to one hour of free exploration with pellet-chasing tasks typically recorded afterward in the same day. Pellet-chasing included the rotation of spatial cues on the curtain during the recording of single unit activity in the small arena to examine whether spatial units remap accordingly, exploration in the small then large arena, and consecutive recordings to examine sleep properties (data not described here).

Behavioural tasks

Spatial alternation

A four-arm cross-shaped wooden maze with raised sides (119 x 119 cm full length; each arm 48 x 23 cm; height 30 cm) was used for the spatial alternation task, allowing the rotation of start points. Each arm could be blocked close to the centre to form a T-maze. In addition, a barrier could be placed within an arm to form a holding area for the start position. Distal spatial cues were available in the recording room including the pulled-back curtain, electrophysiological recording equipment set on wall-mounted shelves, a desk and computer. Animals were first habituated in pairs to the maze and allowed to freely explore for 10 minutes. Rats then individually had two pre-training sessions (5 minutes each) in which they were first placed behind a barrier at the start position at one end of the maze, retained for 10 seconds, then the door removed and the rat allowed to explore the maze. The maze arm opposite to the start was blocked and sucrose pellets (TestDiet 5TUL 20mg, USA) were placed in a shallow dish at the end of each open arm so that they were not visible from the centre of the maze. Rats learnt to run to an arm of the maze to obtain sucrose pellets, which were replaced once they had been consumed and the animal left that arm. The maze was then altered so that a different start arm and blocked arm were used, and another training session run. Each rat had four 5-minute training sessions per day such that each start/blocked configuration was experienced (opposite, adjacent, opposite) for two days initially, with an additional day if required.

For the experiment, rats were placed in the start position for 10 seconds. In each trial there was an initial forced run ('sample'), in which two arms of the cross-shaped maze were blocked forcing the animal into either the left or right arm in order to obtain two sucrose pellets from the end of the arm. The animal was then picked up and returned to the start position and held for approximately 20 seconds before being released for the choice run ('test'), in which one of the barriers was removed from the maze so that the animal had the choice of either the left or right arm (Fig. 2A). Sucrose pellets

were only available in the arm opposite to the sample run, so the rat was rewarded if it alternated. A choice was determined when the back paws of a rat had entered the arm. The rat was then removed from the maze and placed in an open holding cage for 2-3 minutes whilst the maze was rearranged. Each animal had eight sessions consisting of eight trials each, with both the start position and forced turn pseudorandomised so that the same arrangement did not occur more than twice consecutively. Rats were connected to the electrophysiological recording equipment throughout pre-training and each test session.

Bow-tie maze

The bow-tie maze allows continuous object recognition testing, with multiple trials and new novel objects during each session (Albasser et al., 2010). The bow-tie shaped maze had raised sides (wood painted matt black; 120 cm long x 50 cm wide, 50 cm height) and a central sliding. Partitions at each end of the maze split both ends into two short corridors (Fig. 2C). The animals were first habituated to the maze for 10 minutes, by allowing free exploration with sucrose pellets scattered throughout. Next, during the 10 minute session, pellets were first placed in wells at the two ends of the maze and the rat trained to run from one end of the maze to the other when the central door was opened. Then, opaque plastic objects (a funnel and a beaker) were placed behind each baited well. The objects were gradually moved so that they increasingly covering the wells. Rats underwent 4-5 ten minute pre-training sessions, until they readily shuttled across the maze to retrieve sucrose pellets by pushing objects.

For the experimental procedure, 22 pairs of novel objects were used. In the first trial, one novel object was placed covering the sucrose pellets. The rat retrieved the pellets and investigated the object at that end of the maze. After 1 minute, the central door was opened and the rat passed to the opposite end of the maze, where there would be a repeat of the original object (now familiar) and a new novel object (both covering sucrose pellets). This procedure was repeated for all 22 pairs of objects, so that each of the 21 trials consisted of a new novel object and the previous object, which was now familiar (Albasser et al., 2010). Animals were video recorded throughout.

For analysis, the time spent investigating each object was recorded and two measures of recognition, D1 and D2, were calculated (Albasser et al., 2010). D1 represents the difference in exploration time between novel and familiar objects, and is calculated by subtracting the time spent exploring a familiar object from the time spent exploring a novel object. Cumulative D1 represents the sum of the exploration time for all novel objects minus the sum of exploration time for all familiar objects across all trials. D2 represents the total difference in exploration time (cumulative D1) divided by the total exploration time for both novel and familiar objects, resulting in a ratio that ranges between +/- 1.

Transient inactivation of the ATN (muscimol)

An additional cohort (n=6, ATNmusc) was implanted with bilateral infusion guide cannulae (26 gauge, 4mm length; Bilaney Consultants Ltd., UK) aimed at the ATN at an angle of 28.6° towards the midline (AP -1.7mmg, ML ±3.6mm, DV -4.0mm from top of cortex) alongside subiculum electrode implantation. A dummy cannula (0.203mm diameter, 4mm length; Bilaney Consultants Ltd., UK) was use to protect each guide cannula during recovery and normal recording activity. All other surgical and electrophysiological methods were the same as those used for the animals with permanent ATN lesions.

Following recovery, rats were trained daily for a minimum of one week prior to commencing inactivation experiments. Rats were lightly restrained and the dummy cannulae removed and replaced several times. During this period, rats were also trained in the spatial alternation (T-maze) task and

electrophysiological activity was recorded during free exploration and pellet-chasing in the large and small square arenas. All apparatus matched that used for the ATNx rats.

On the day of experimentation, electrophysiological recordings of exploration and pellet-chasing were first performed pre-infusion for 20-40 minutes to establish a baseline. The animal was then lightly restrained and muscimol (concentration 0.5mg / 1ml saline) infused through a 33gauge infusion needle with a 1- or 2mm projection past the length of the implanted guide cannula, targeting the ATN. Muscimol was infused over 90 seconds using a 0.5µl Hamilton syringe and infusion pump (KD Scientific, Hollister, USA). The infusion needle was retained in position for a further 60 seconds before it was removed and replaced with the dummy cannula. Rats received a 0.2µl at each of two locations per hemisphere using both a 5- and 6mm length infusion needle in order to target the whole ATN (Fig. 1H). Following infusion, electrophysiological recordings during pellet-chasing and exploration were conducted in consecutive 20 minute sessions in the small and large square arena. Between 90 and 120 minutes into the experiment, the T-maze task was performed (8 trials, pseudo-randomised starting points). Animals were then returned to the square arena and recorded for a further 2-3 hours, including during sleep. Regular diet and water were freely available in the recording arena after the T maze test. The following day, further electrophysiological recordings were undertaken to determine whether the effects of muscimol had ceased and cell activity had returned to baseline.

Muscimol infusions were repeated 1-2 weeks after the initial experiment. In two cases, an additional control infusion of saline was given. In order to visualise the location of the muscimol infusion, the tracer fluorogold (Sigma-Aldrich Ireland Ltd, Ireland) was infused one day prior perfusion.

Perfusion and histology

After completion of experiments, animals were sacrificed and perfused transcardially with 0.1M phosphate buffered saline (PBS) then 2.5% paraformaldehyde (PFA) in 0.1M PBS. Brains were removed and post-fixed in PFA for 24 hours then transferred to 30% sucrose in 0.1M PBS solution for 2 days. A cryostat (Leica CM1850) was used to cut 40µm sections in a 1:4 series. One series was mounted onto double gelatin-subbed microscope slides and, once completely dry, washed in decreasing concentration of alcohol (100, 90, 70%) before being stained with cresyl violet, a Nissl stain (Sigma-Aldrich Ireland Ltd, Ireland). Sections were then dehydrated with increasing alcohol concentrations, washed in xylene, and cover-slipped.

Of the other series, one was reacted against anti-calbindin antibody raised in mouse (Sigma-Aldrich Ireland Ltd, Ireland) and another against anti-NeuN antibody raised in mouse (Sigma-Aldrich Ireland Ltd, Ireland). The remaining series was reacted with either anti-parvalbumin antibody raised in mouse (Sigma-Aldrich Ireland Ltd, Ireland) or, in the temporary inactivation cohort, with anti-fluorogold raised in rabbit (EMD Millipore, USA).

In brief, sections were washed in a quench solution (10% methanol and 0.3% hydrogen peroxide in distilled water) before PBS (0.1M pH 7.35) then PBST (2ml Triton X-1000 in 1 litre 0.1M PBS; pH 7.35) washes. Sections were stirred for one hour in 4% normal horse serum in PBST before the primary antibody was added (1:5000 dilution in PBST for calbindin, parvalbumin and fluorogold; 1:10000 for NeuN) and stirred at 4° overnight. Sections were then washed in PBST before being incubated for two hours in 1:250 dilution of horse-anti-mouse (Vector Labs, UK), or, in the case for fluorogold, horse-anti-rabbit (Vector Labs, UK), in PBST. After further PBST washes sections were incubated at room temperature in Vectastain ABC Solution (Vector Labs, UK) before further PBST and PBS washes. Sections were then reacted with DAB solution (Vector Labs, UK) and washed in PBS.

All sections were mounted on double-subbed slides, and fluorogold reacted slides were lightly stained with cresyl violet for improved tissue visualisation before coverslipping. Sections were imaged using either an Olympus BX51 upright microscope or Leica Aperio AT2 slidescanner.

Image analysis

Individual images of sections were aligned and tiled using Inkscape (http://inkscape.org) and FIJI (**F**iji **I**s **J**ust **I**mage J, https://imagej.net/Fij, Schindelin et al 2013[3]). Cresyl violet stained sections helped to confirm electrode placement. In order to assess lesion success, the ATN was segmented from photomicrographs of anti-NeuN reacted sections using FIJI and the resulting image thresholded to show nuclei separation, before using the inbuilt Analyse Particles plugin to obtain a cell count. The ATN cell counts were compared between the ATNx, Normal and Sham control groups to determine lesion effectiveness. Calbindin-reacted sections helped to determine the status of nucleus reuniens.

Recording and Statistical Analysis

Unit identification and isolation

Unit identification used the following criteria: units had to be active, and show consistent waveform characteristics (amplitude, height, and duration) during recording, as well as a clean refractory period (>2 ms) in the inter-spike interval (ISI) histogram. Spike amplitude was measured as the difference between the positive peak and first negative peak before the positive peak, if present, or zero. Spike height was the difference between the spike peak to the minimum value of the spike waveform. Spike width was the distance in microseconds beyond which the waveform drops below 25% of its peak value.

Units were sometimes seemingly recorded for more than for 1 day, despite electrode lowering. For these cases, cells were monitored on the relevant tetrodes from day-to-day; for analysis, only clean recordings with the largest sample size and spikes of the highest amplitude were chosen. Particular care was taken to exclude seemingly-related samples from analysis to avoid inadvertent double-counting of cells. During spike sorting, the signals from each cell were carefully followed from first appearance to complete loss, to avoid overestimation of cell counts. Additionally, any ambiguous sessions were rejected. Once well-defined neuronal signals were isolated recording commenced. For permanent lesion experiments, rats had to explore at least 90% of the open field in a session to be included in analyses to allow reliable calculation of spatial characteristics.

Statistical Analysis and Unit Classification

Units were sorted using conventional cluster-cutting techniques (Tint, Axona Ltd.). Standard statistical testing was performed using an open-source custom-written suite in Python (NeuroChaT; Islam et al., 2019); additional custom codes in R, and Axona. Units were classified based on the spatiotemporal features of their activity in the open field during pellet-chasing, as described below.

Spatial Analyses

Additional analyses examined spatial modulation of recorded units. Multiple indices were used to analyse the spatial properties of unit activity (namely spatial coherence, spatial information content, and spatial reliability). A firing field was defined as a set of at least nine contiguous pixels with firing rate above zero. A place field was identified if nine neighbouring pixels (sharing a side) were above 20% of the peak firing rate. Place field size was represented by number of pixels. Spatial specificity (spatial information content) was expressed in bits per spike (Skaggs et al., 1996). The spatial selectivity of a firing field (ratio of maximal signal to noise) was calculated by dividing the firing rate of

the cell in the bin with the maximum average rate by its mean firing rate over the entire apparatus (Skaggs et al., 1996). Mean frequency is the total number of spikes divided by the total recording time and is expressed in Hz. Exploration was assessed by comparing the occupancy of bins and the number of visits per bin during recording sessions. Additionally, to be regarded as place cells, the following criteria had to be met: all included as place cells had to have a spatial information content (Skaggs et al., 1996) index of > 0.5; a spatial coherence of > 0.25; and a mean firing rate > 0.25. The spatial path of the subject and the spike train are used to produce a locational firing rate map. To determine the existence of a hexagonal grid firing structure, grid index, size and orientation were calculated. The grid cell analysis involves calculating the spatial autocorrelation of the firing rate map and assessing the shape formed by the peaks in autocorrelation. For border cell analyses, a border of the arena is estimated from the path the animal traversed and the firing rate is compared to the distance from the border.

Bursting analysis

Bursting units were identified using criteria based on Anderson and O'Mara (2003). A burst was defined as a series of spikes in which each inter-spike interval (ISI) was minimum of 10ms, and contained a minimum of two spikes, with a minimum inter-burst interval (IBI) of 50ms. Further bursting analyses examined the total number of burst during a recording session; the number of spikes in the bursting cluster; mean inter-spike interval during the burst cluster; number of spikes per burst; burst duration; duty cycle (the portion of an inter-burst interval during which a burst fires); the inter-burst interval; and propensity to burst, calculated by dividing the number of bursting spikes by the total number of spikes in a recording.

Acknowledgements: This work was supported by a Joint Senior Investigator Award made by The Wellcome Trust to JPA (103722/Z14/Z) and SMOM.

Author contributions:

BEF: Acquisition of data, analysis and interpretation of data, drafting or revising the article;

SKM: Developing analysis algorithms, Python script writing and validation, analysis and interpretation of data, drafting or revising the article

MNI: Original conception and development of NeuroChaT

JPA, SMOM: Conception and design, analysis and interpretation of data, drafting and revising the article

Declaration of interests: The authors declare that no competing financial or non-financial interests exist.

References

Aggleton, J. P. (2005). Cognitive deficits induced by lesions of structures containing head direction cells. In Head direction cells and the neural mechanisms of spatial orientation. Eds S.I. Wiener and J.S. Taube. MIT Press, Cambridge MA, pp 275-296.

Aggleton, J. P. and Brown, M. W. (1999). Episodic memory, amnesia, and the hippocampal–anterior thalamic axis. Behav. Brain Sci. 22, 425-444.

Aggleton, J. P., Keith, A. B., and Sahgal, A. (1991). Both fornix and anterior thalamic, but not mammillary, lesions disrupt delayed non-matching-to-position memory in rats. Behav.Brain Res. 44, 151-161.

Aggleton, J. P., Neave, N., Nagle, S., and Hunt, P. R. (1995). A comparison of the effects of anterior thalamic, mammillary body and fornix lesions on reinforced spatial alternation. Behav. Brain Res. 68, 91-101.

Aggleton, J. P. and Nelson, A. J. (2015). Why do lesions in the rodent anterior thalamic nuclei cause such severe spatial deficits? Neurosci. Biobehav. Rev. 54, 131-144.

Albasser, M. M., Chapman, R. J., Amin, E., Iordanova, M. D., Vann, S. D., and Aggleton, J. P. (2010). New behavioural protocols to extend our knowledge of rodent object recognition memory. Learn. Mem. 17), 407-419.

Albo, Z., Di Prisco, G. V., & Vertes, R. (2003). Anterior thalamic unit discharge profiles and coherence with hippocampal theta rhythm. *Thalamus & Related Systems*, *2*(2), 133-144.

Amaral, D. G., Dolorous, C. and Alvarez-Roy, P. (1991). Organisation of CA1 projections to the subiculum: a PHA-L analysis in the rat. Hippocampus 1, 415–436.

Anderson, M. I., and O'Mara, S. M. (2003). Analysis of recordings of single-unit firing and population activity in the dorsal subiculum of unrestrained, freely moving rats. J. Neurophys. 90(2), 655-665.

Anderson, M. I. and O'Mara, S. M. (2004). Responses of dorsal subicular neurons of rats during object exploration in an extended environment. Exp Brain Res, 159, 519-529.

Boccara, C. N., Sargolini, F., Thoresen, V. H., Solstad, T., Witter, M. P., Moser, E. I. and Moser, M. B. (2010). Grid cells in pre-and parasubiculum. Nat Neurosci, 13(8), 987-994.

Bonnevie T., Dunn B., Fyhn M., Hafting T., Derdikman D., Kubie J. L., Roudie Y., Moser E. I., Moser M. B. (2013). Grid cells require excitatory drive from the hippocampus. Nat Neurosci, 16(3), 309-317.

Brotons-Mas, J. R., Montejo, N., O'Mara, S. M., and Sanchez-Vives, M. V. (2010). Stability of subicular place fields across multiple light and dark transitions. Eur. J. Neurosci. 32, 648-658.

Brotons-Mas, J. R., Schaffelhofer, S., Guger, C., O'Mara, S. M., and Sanchez-Vives, M. V. (2017). Heterogeneous spatial representation by different subpopulations of neurons in the subiculum. Neurosci. 343, 174-189.

Byatt, G., and Dalrymple-Alford, J. C. (1996). Both anteromedial and anteroventral thalamic lesions impair radial-maze learning in rats. Behav. Neurosci. 110, 1335 - 1348.

Calton, J. L., Stackman, R. W., Goodridge, J. P., Archey, W. B., Dudchenko, P. A., and Taube, J. S. (2003). Hippocampal place cell instability after lesions of the head direction cell network. J. Neurosci. 23, 9719-9731.

Cembrowski, M. S., Phillips, M. G., DiLisio, S. F., Shields, B. C., Winnubst, J., Chandrashekar, J., Bas, E. and Spruston, N. (2018). Dissociable structural and functional hippocampal outputs via distinct subiculum cell classes. Cell, 173(5), 1280-1292.

Clark, B. J., and Harvey, R. E. (2016). Do the anterior and lateral thalamic nuclei make distinct contributions to spatial representation and memory? Neurobiol. Learn.Mem. 133, 69-78.

Davidson, T. L. and Jarrard, L .E. (2004). The hippocampus and inhibitory learning: a 'Gray'area? Neurosci. Biobehav. Rev. 28(3), 261-271.

Deadwyler, S. A. and Hampson, R. E. (2004). Differential but complementary mnemonic functions of the hippocampus and subiculum. Neuron, 42(3), 465-476.

Dillingham, C. M., Milczarek, M. M., Perry, J. C., Frost, B. E., Parker, G. D., Assaf, Y., Sengpiel, F., O'Mara, S. M., and Vann, S. D. (2019). Mammillothalamic disconnection alters hippocampo-cortical oscillatory activity and microstructure: Implications for diencephalic amnesia. J. Neurosci. 39(34), 6696-6713.

Dillingham, C. M., & Vann, S. D. (2019). Why isn't the head-direction system necessary for direction? Lessons from the lateral mammillary nuclei. Front. Neural Circ. 13, 60.

Dudchenko, P. A., Muir, G. M., Frohardt, R. J., and Taube, J. S. (2005). What does the head direction cell system really do? In Head Direction Cells and the Neural Mechanisms of Spatial Orientation, eds. S.I Wiener, J.S. Taube. MIT press, Cambridge, MA, pp. 221-245.

Dumont, J. R. and Aggleton, J. P. (2013). Dissociation of recognition and recency memory judgments after anterior thalamic nuclei lesions in rats. Behav Neurosci, 127(3), 415-431.

Ferguson, M. A., Lim, C., Cooke, D., Darby, R. R., Wu, O., Rost, N. S., Corbetta, M., Grafman, J. and Fox, M. D. (2019). A human memory circuit derived from brain lesions causing amnesia. Nature Comms. 10, 1-9.

Goodridge, J. P. and Taube, J. S. (1997). Interaction between the postsubiculum and anterior thalamus in the generation of head direction cell activity. J. Neurosci. 17, 9315-9330.

Gray, J. A. and McNaughton, N. (1983). Comparison between the behavioural effects of septal and hippocampal lesions: a review. Neuroscience & Biobehavioral Reviews, 7(2), 119-188.

Hafting, T., Fyhn, M., Molden, S., Moser, M. B. and Moser, E. I. (2005). Microstructure of a spatial map in the entorhinal cortex. Nature, 436(7052), 801–806.

Haugland, K. G., Sugar, J. and Witter, M. P. (2019). Development and topographical organization of projections from the hippocampus and parahippocampus to the retrosplenial cortex. Eur. J. Neurosci. 50, 1799-1819.

Henry, J., Petrides, M., St-Laurent, M. and Sziklas, V. (2004). Spatial conditional associative learning: effects of thalamo-hippocampal disconnection in rats. Neuroreport 15, 2427-2431.

Jankowski, M. M., Islam, M. N., Wright, N. F., Vann, S. D., Erichsen, J. T., Aggleton, J. P., and O'Mara, S. M. (2014). Nucleus reuniens of the thalamus contains head direction cells. Elife, 3, e03075.

Jankowski, M. M., Passecker, J., Nurul Islam, M D., Vann, S. D., Erichsen, J., Aggleton, J. P., O'Mara, S. M. (2015). Evidence for spatially-responsive neurons in the rostral thalamus. Front. Behav. Neurosci. doi: 10.3389/fnbeh.2015.00256

Jung, H. Y., Staff, N. P., and Spruston, N. (2001). Action potential bursting in subicular pyramidal neurons is driven by a calcium tail current. J. Neurosci., 21(10), 3312-3321.

Lee, I., Yoganarasimha, D., Rao, G., and Knierim, J. J. (2004). Comparison of population coherence of place cells in hippocampal subfields CA1 and CA3. Nature 430, 456-459.

Lever, C., Burton, S., Jeewajee, A., O'Keefe, J., and Burgess, N. (2009). Boundary vector cells in the subiculum of the hippocampal formation. J. Neurosci. 29, 9771-9777.

Matulewicz, P., Ulrich, K., Islam, M. N., Mathiasen, M. L., Aggleton, J. P., and O'Mara, S. M. (2019). Proximal perimeter encoding in the rat rostral thalamus. Sci. Reports 9, 2865.

Moran, J. P. and Dalrymple-Alford, J. C. (2003). Perirhinal cortex and anterior thalamic lesions: comparative effects on learning and memory. Behav. Neurosci. 117, 1326-1341.

Morris, R. G., Garrud, P., Rawlins, J. A., and O'Keefe, J. (1982). Place navigation impaired in rats with hippocampal lesions. Nature 297, 681-683.

Moser, E. I., Kropff, E., and Moser, M. B. (2008). Place cells, grid cells, and the brain's spatial representation system. Ann. Rev. Neurosci. 31, 69-89.

Nitzan, N., McKenzie, S., English, D. F., Beed, P., Oldani, S., Tukker, J. J., Buzsáki, G. and Schmitz, D., (2019). Propagation of Hippocampal Ripples to the Neocortex by Way of a Subiculum-Retrosplenial Pathway. NEURON-D-19-00544. Available at SSRN: https://ssrn.com/abstract=3381954 or http://dx.doi.org/10.2139/ssrn.3381954

O'Keefe, J. (1979). A review of the hippocampal place cells. Progr. Neurobiol. 13, 419-439.

O'Mara, S. (2005). The subiculum: what it does, what it might do, and what neuroanatomy has yet to tell us. J Anatomy, 207(3), 271-282.

O'Mara, S. M., Sanchez-Vives, M. V., Brotons-Mas, J. R., and O'Hare, E. (2009). Roles for the subiculum in spatial information processing, memory, motivation and the temporal control of behaviour. Prog. Neuro-Psychopharm. Biol. Psych. 33(5), 782-790.

O'Mara, S. M., Commins, S., Anderson, M. and Gigg, J. (2001). The subiculum: a review of form, physiology and function. Prog. Neurobiol. 64, 129-155.

O'Mara, S. M. and Aggleton, J. (2019). Space and Memory (Far) Beyond the Hippocampus: Many Subcortical Structures Also Support Cognitive Mapping and Mnemonic Processing. Front. Neural Circ, 13, 52. doi: 10.3389/fncir.2019.00052

Perry, B. A., Mercer, S. A., Barnett, S. C., Lee, J., and Dalrymple-Alford, J. C. (2018). Anterior thalamic nuclei lesions have a greater impact than mammillothalamic tract lesions on the extended hippocampal system. Hippocampus, 28, 121-135.

Poirier, G .L. and Aggleton, J. P. (2009). Post-surgical interval and lesion location within the limbic thalamus determine extent of retrosplenial cortex immediate-early gene hypoactivity. Neurosci, 160(2), 452-469.

Ranganath, C., and Ritchey, M. (2012). Two cortical systems for memory-guided behaviour. Nat. Rev. Neurosci. 13, 713-726.

Schindelin J., Arganda-Carreras I., Frise E., Kaynig V., Longair M., Pietzsch T., Preibisch S., Rueden C., Saalfeld S., Schmid B., Tinevez J. Y., White D. J., Hartenstein V., Eliceiri K., Tomancak P., Cardona A. (2013). Fiji: an open-source platform for biological-image analysis. Nat. Methods 9(7), 676-682.

Sharp, P. E. and Green, C. (1994). Spatial correlates of firing patterns of single cells in the subiculum of the freely moving rat. J. Neurosci. 14, 2339-2356.

Shibata, H. (1993). Direct projections from the anterior thalamic nuclei to the retrohippocampal region in the rat. J. Comp. Neurol. 337, 431-445.

Spiers, H. J., Maguire, E. A. and Burgess, N. (2001). Hippocampal amnesia. Neurocase 7, 357-382.

Staff, N. P., Jung, H. Y., Thiagarajan, T., Yao, M., and Spruston, N. (2000). Resting and active properties of pyramidal neurons in subiculum and CA1 of rat hippocampus. J Neurophys, 84, 2398-2408.

Stewart, M. and Wong, R. K. (1993). Intrinsic properties and evoked responses of guinea pig subicular neurons in vitro. J Neurophys, 70, 232-245.

Sutherland, R. J., and Rodriguez, A. J. (1989). The role of the fornix/fimbria and some related subcortical structures in place learning and memory. Behav. Brain Res. 32, 265-277.

Taube, J. S. (1995). Head direction cells recorded in the anterior thalamic nuclei of freely moving rats. J. Neurosci. 15, 70-86.

Taube, J. S. (2007). The head direction signal: origins and sensory-motor integration. Annu. Rev. Neurosci. 30, 181-207.

Tsanov, M., Chah, E., Vann, S. D., Reilly, R. B., Erichsen, J. T., Aggleton, J. P., and O'Mara, S. M. (2011). Theta-modulated head direction cells in the rat anterior thalamus. J. Neurosci. 31, 9489-9502.

van Groen, T. and Wyss, J. M. (1990). The connections of presubiculum and parasubiculum in the rat. Brain Res. 518(1-2), 227-243.

van Groen, T., Kadish, I., and Wyss, J. M. (2002). Role of the anterodorsal and anteroventral nuclei of the thalamus in spatial memory in the rat. Behav. Brain Res., 132(1), 19-28.

Vann, S. D. (2005). Transient spatial deficit associated with bilateral lesions of the lateral mammillary nuclei. Eur. J. Neurosci. 21, 820-824.

Vann, S. D. (2018). Lesions within the head direction system reduce retrosplenial c-fos expression but do not impair performance on a radial-arm maze task. Behav. Brain Res. 338, 153-158.

Vann, S. D., and Aggleton, J. P. (2004). The mammillary bodies: two memory systems in one? Nat. Rev. Neurosci. 5, 35-44.

Van Strien, N. M., Cappaert, N. L. M., and Witter, M. P. (2009). The anatomy of memory: an interactive overview of the parahippocampal–hippocampal network. Nat. Rev. Neurosci. 10, 272-282.

Warburton, E. C. and Aggleton, J. P. (1999). Differential deficits in the Morris water maze following cytotoxic lesions of the anterior thalamus and fornix transection. Behav. Brain Res. 98, 27-38.

Warburton, E. C., Morgan, A., Baird, A. L., Muir, J. L. and Aggleton, J. P. (1999). Does pretraining spare the spatial deficit associated with anterior thalamic damage in rats? Behav. Neurosci. 113(5), 956-967.

Warburton, E. C., Baird, A. L., Morgan, A., Muir, J. L., and Aggleton, J. P. (2000). Disconnecting hippocampal projections to the anterior thalamus produces deficits on tests of spatial memory in rats. Eur. J. Neurosci. 12, 1714-1726.

Warburton, E. C., Baird, A., Morgan, A., Muir, J. L., and Aggleton, J. P. (2001). The conjoint importance of the hippocampus and anterior thalamic nuclei for allocentric spatial learning: evidence from a disconnection study in the rat. J. Neurosci. 21, 7323-7330.

Winter, S. S., Clark, B. J., and Taube, J. S. (2015). Disruption of the head direction cell network impairs the parahippocampal grid cell signal. Science, 347, 870-874.

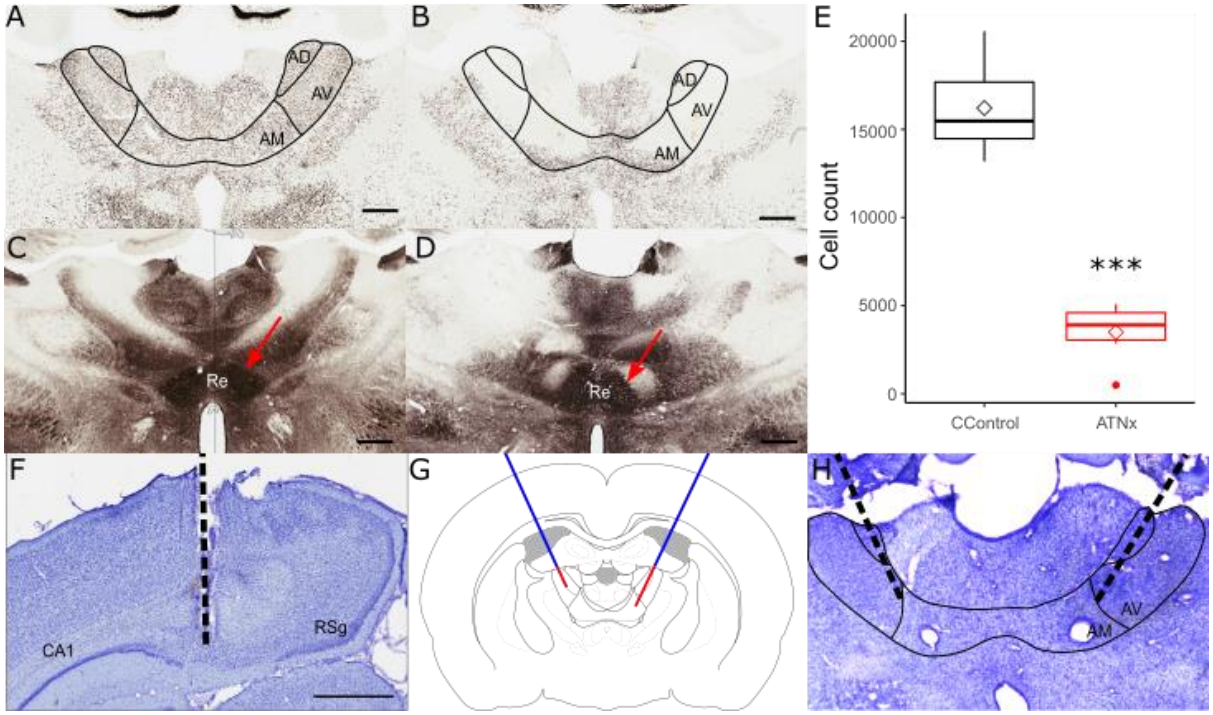

Fig 1: NeuN-reacted coronal sections showing status of the anterior thalamic nuclei (ATN) in control (A) and lesion (B) animals. The nucleus reuniens (arrowed), as shown using calbindin-reacted sections, was intact in both control (C) and lesion (D) animals, indicating that reuniens damage was not responsible for deficits seen in ATN lesioned animals. (E) The ATN cell count was significantly reduced in lesioned animals (ATNx) compared to controls (CControl). Nissl-stained coronal sections helped to confirm electrode placement in dorsal subiculum (F), with the electrode path indicated. (G) Schematic representing cannula placement (blue) and the two targets of the infusion needle (red). (H) Cresyl violet stained section indicating cannula placement, with DAB-reacted flurogold infused to indicate spread of muscimol. *** = $p<0.001$ (Welch's Two Sample *t*-test). Scale bar = 800µm

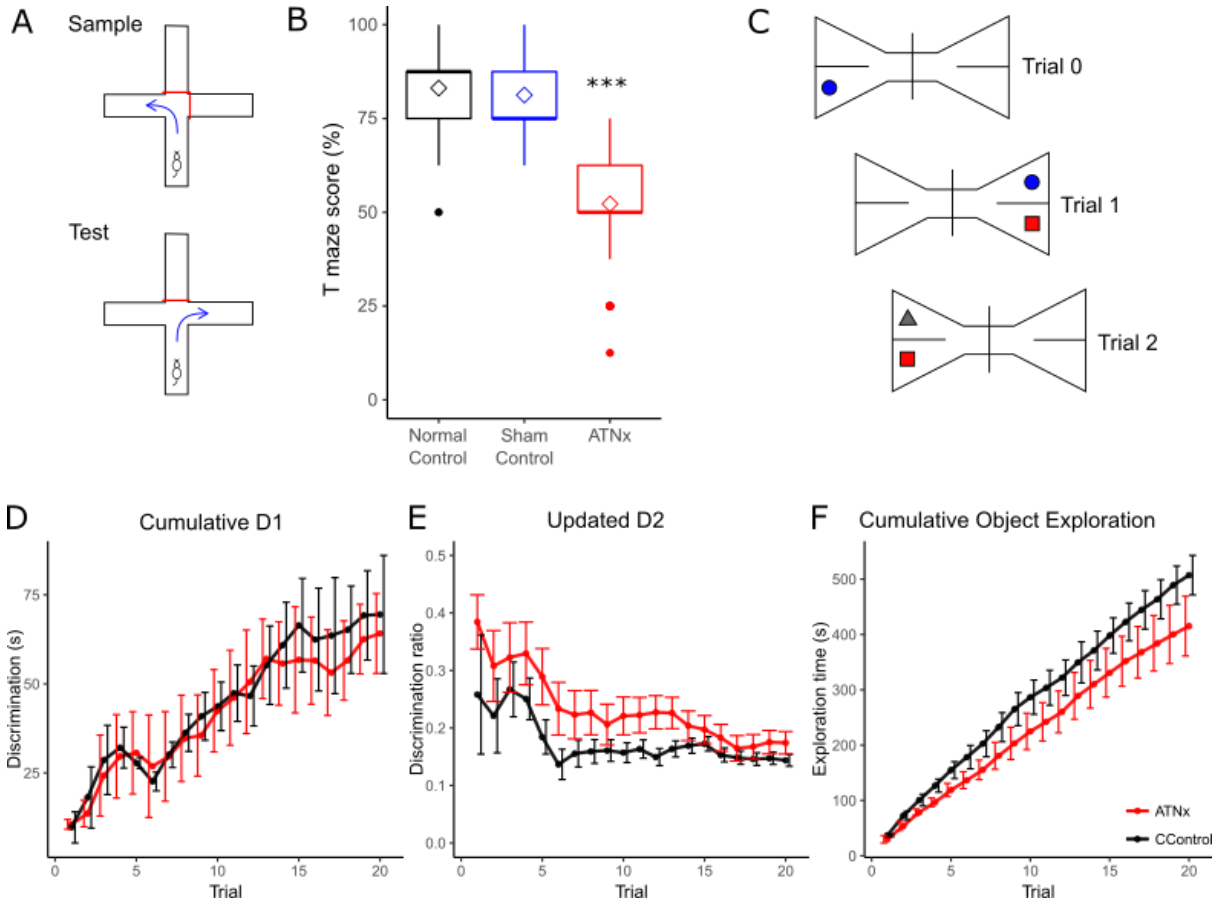

Fig 2: (A) Schematic diagram of spatial alternation task. ATN lesioned animals (ATNx) showed a significant deficit in spatial alternation compared to both control and sham animals (B). (C) Schematic of novel object recognition task. There was no difference between control (CControl) and lesion rats in cumulative D1 (D), D2 (E), or total exploration time (F). *** $p<0.001$.

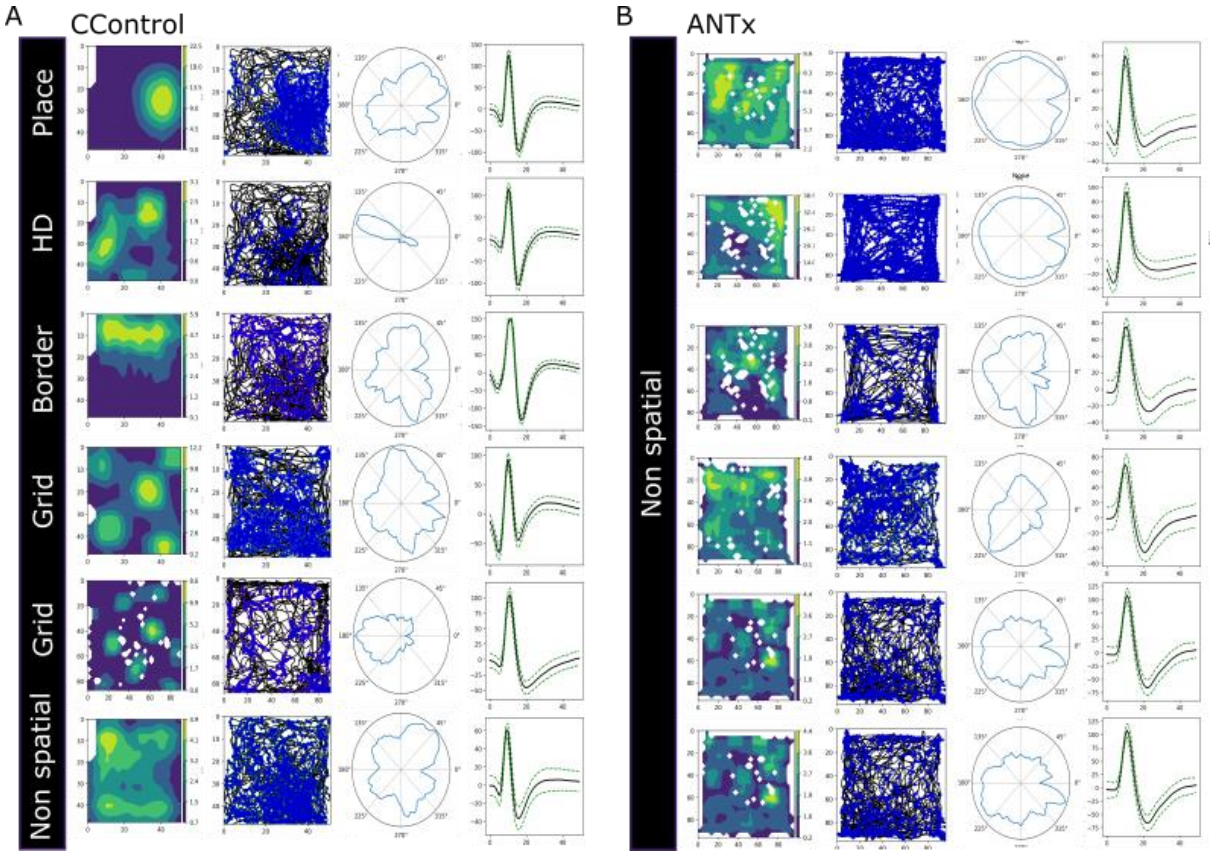

Fig 3: Representative single units recorded in the dorsal subiculum in control (CControl; A) and ATN lesion (ATNx; B) animals. For individual units the figures illustrate: Heatmap of spike location adjusted for time spent in each location; path in arena (black) with spike location (blue); head direction; mean spike waveform. For the CControl group, different classes of spatial cells are displayed, along with a non-spatial cell. No spatial cells were recorded in the ATNx cases. HD, head direction.

	Control		Lesion	
	Mean	**± SD**	**Mean**	**± SD**
Number of spikes (per 20 minutes)	2633.47	2936.55	4914.12	6982.46
Spiking frequency (Hz)	2.76	3.85	5.36	7.24
Spike amplitude (μV)	110.68	33.66	102.67	20.24
Spike height (μV)	153.89	60.07	157.11	38.21
Spike width (ms) ***	149.25	46.75	208.37	51.43
Inter-spike interval (ISI; ms)	917.05	1235.86	2296.00	3249.80
Total bursts (per 20 minutes)	142.53	295.58	246.64	526.18
Total bursting spikes (per 20 minutes)	314.13	663.72	528.96	1136.20
Mean bursting ISI (ms)	4.11	0.41	3.88	0.48
Spikes per burst *	2.15	0.14	2.08	0.12
Mean burst duration (ms) *	5.71	0.75	5.22	0.76
Inter-burst interval (ms) *	28074.20	44912.37	78167.00	99288.27
Mean duty cycle (burst duration / inter-burst interval)	0.06	0.06	0.02	0.03
Propensity to burst (bursting spikes / total spikes) ***	0.10	0.08	0.05	0.05

Table 1: Summary of spike and burst properties of subicular units. Duty cycle describes the portion of the inter-burst interval during which a burst fires. * $p<0.05$, ** $p<0.01$, *** $p<0.001$.

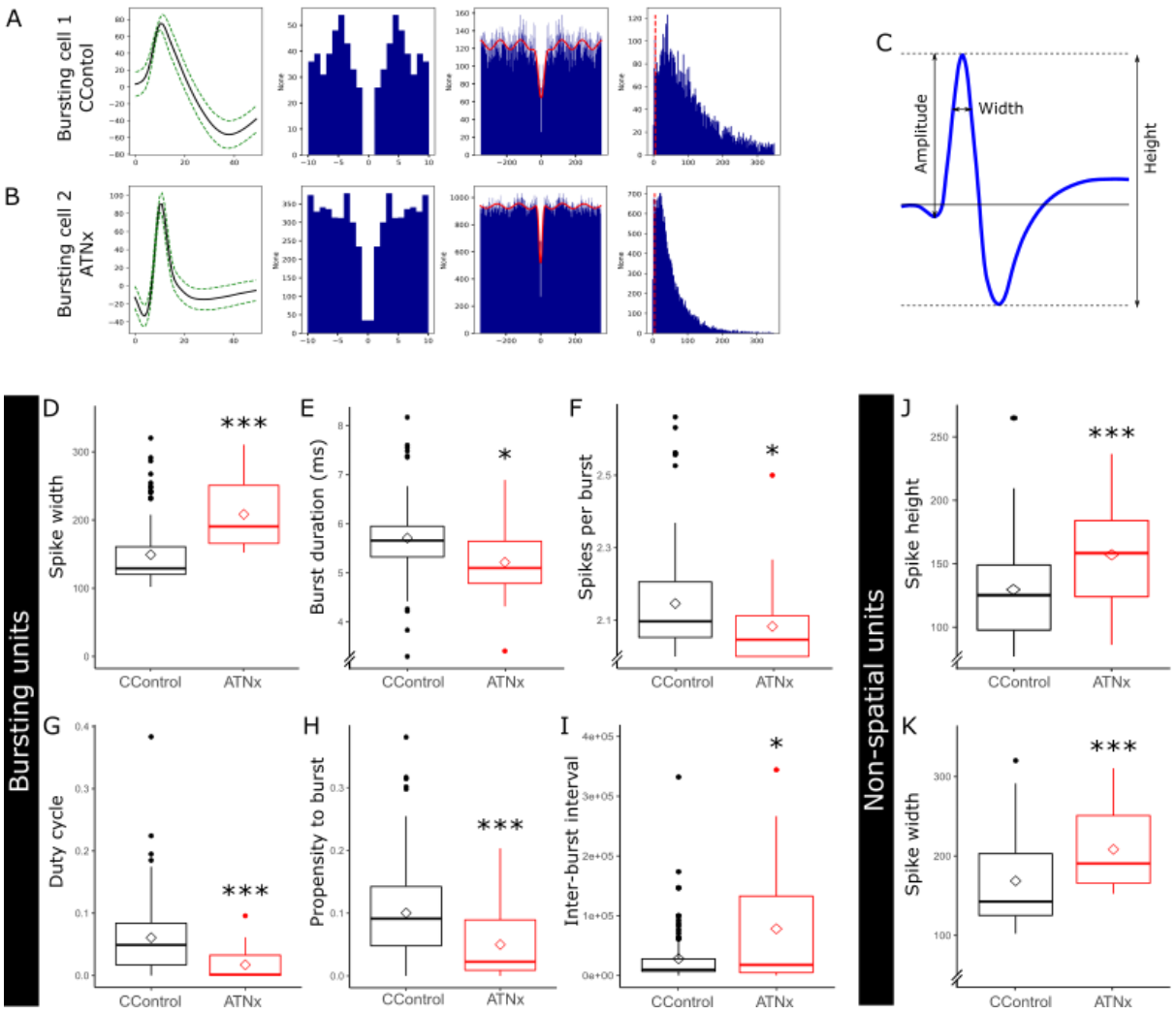

Fig 4: Properties of bursting and non-spatial subicular cells. (A, B) Waveforms and autocorrelation histograms were used for cell classification. (C)Diagram of waveform properties. Bursting cells in CControl showed a higher burst duration (E), had more spikes per burst (F), and had a higher propensity to burst (H). Bursting cells in ATNx had a greater spike width (D) and higher inter-burst interval (I), than non-bursting cells. (J, K) Non-spatial cells in ATN had higher spike width and spike height than non-spatial cells in CControl animals. For boxplots (D-K), filled circles indicate outliers and unfilled diamonds indicate the mean. * p<0.05, ** p<0.01, *** p<0.001.

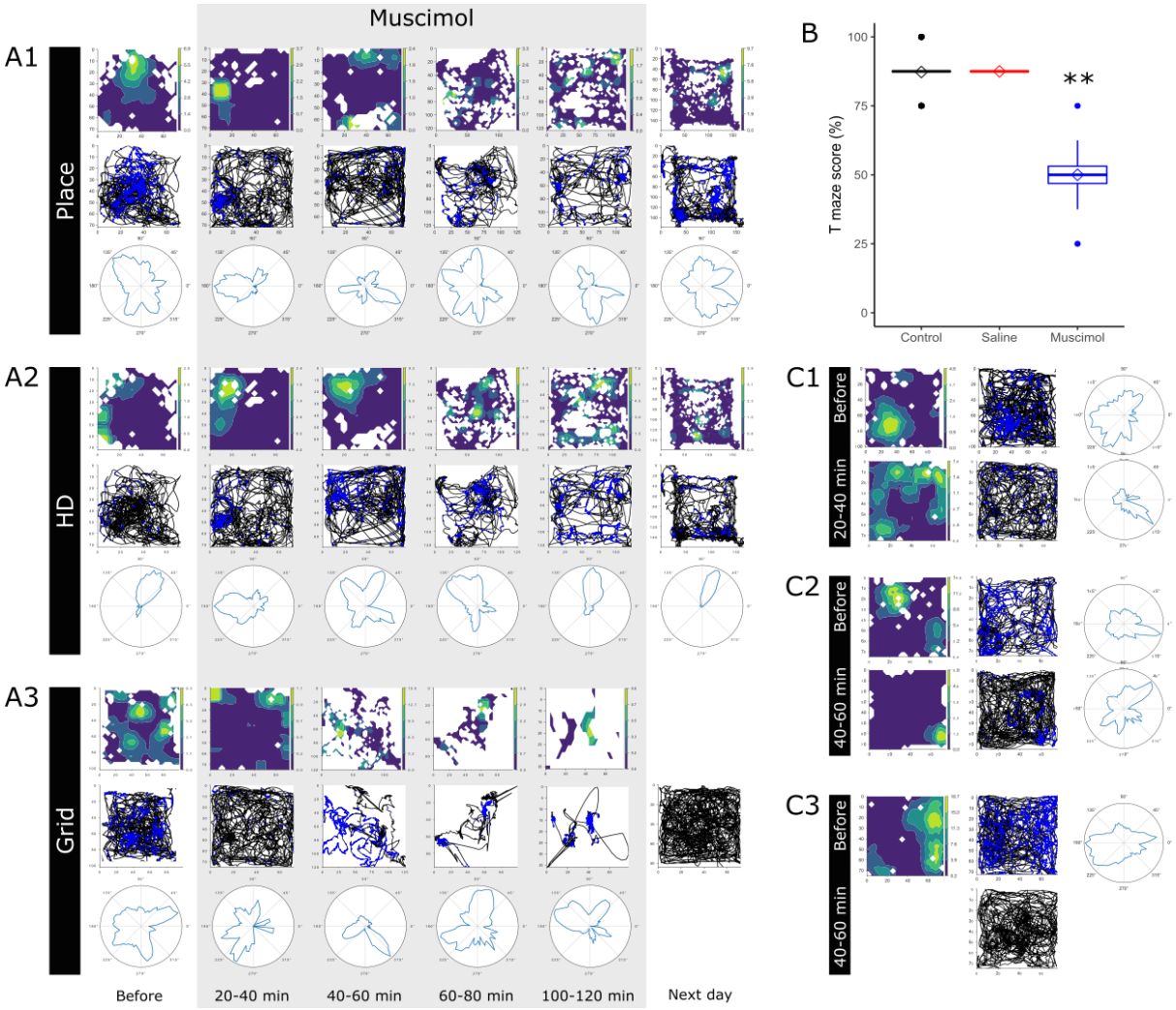

Fig 5: (B) Spatial alternation dropped to chance levels when the ATN were temporarily inactivated with muscimol, compared to the same animals prior to infusion. When saline was infused in place of muscimol no deficit was present. (A1-A3) Examples of spatial units before, during and after muscimol infusion. Spatial properties of single units decreased when ATN was inactivated. (Note, unit A3 showed relative inactivity after 100-120 minutes, and the cell was not recorded the next day). (C1-C3) further examples of spatial units before and after ATN inactivation. C1 shows disruption of place field shortly after muscimol infusion with some head directionality remaining, which was later disrupted. For (C3), no firing was detected after muscimol infusion. ** = $p<0.01$.

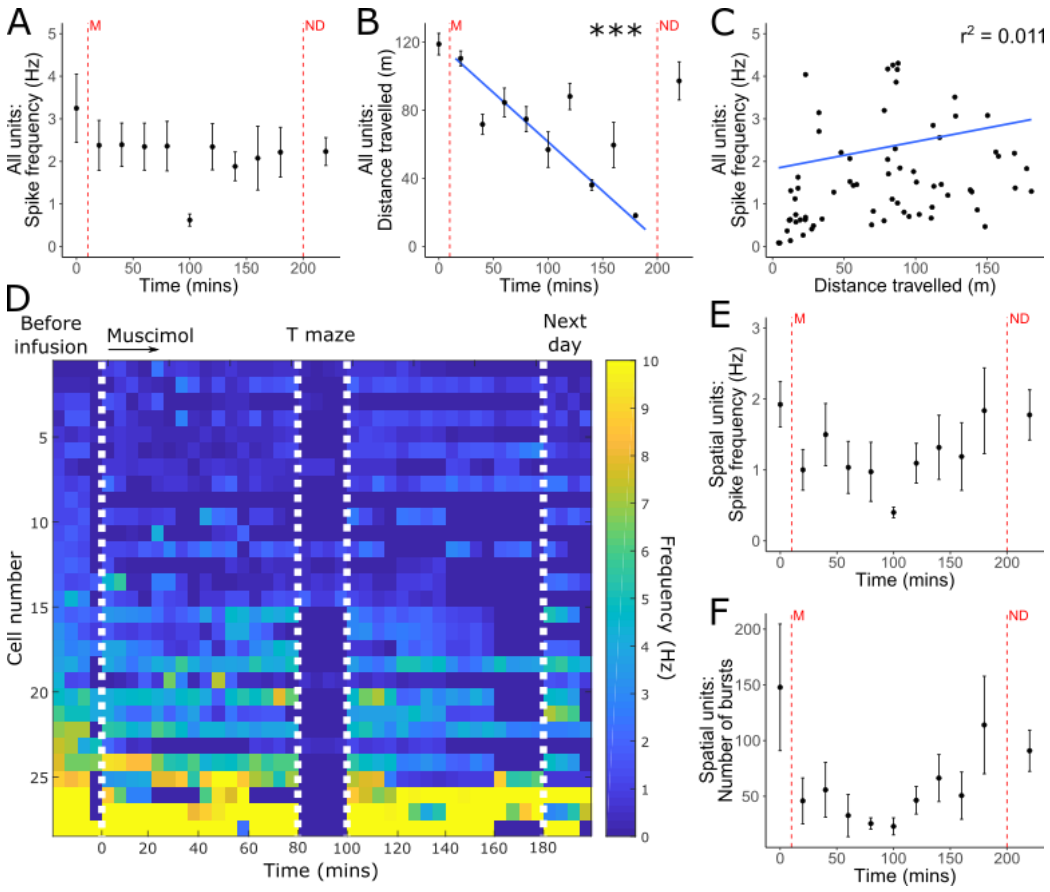

Fig 6: Spike properties following temporary inactivation of ATN with muscimol (M). (A) Inactivation of ATN caused no significant decrease in single unit firing frequency. (B) Animals showed decreasing levels of activity throughout the experiment, although there was no significant correlation between distance travelled and spike frequency (C). (D) Represents firing frequency of each cell recorded at baseline (left), in 5 minute bins throughout the experiment. The first white line indicates ATN inactivation with muscimol, after 15-20 minutes of baseline recording before infusion. In most cases, electrophysiological recording was paused for T maze between 80-100 minutes (second and third white lines), then continued. Recordings in which the animal was largely inactive or asleep were excluded. The final white line indicates data from the day after infusion. (E) There were no significant changes in spike firing in spatial units as a result of ATN inactivation and burst properties remained consistent including number of burst (F). (A, B, E, F) First red vertical line ('M') indicates the infusion of muscimol, second red vertical line indicates recordings taken the next day ('ND'). Each bin represents 20 minutes of recording. Data are compared to baseline, immediately prior to inactivation, with error bars indicating SEM. Theta entrained cells are removed from A, B and C due to high firing frequency compared to other cell classes. *** $p<0.001$ (Welch's Two Sample *t*-test with Bonferroni correction).

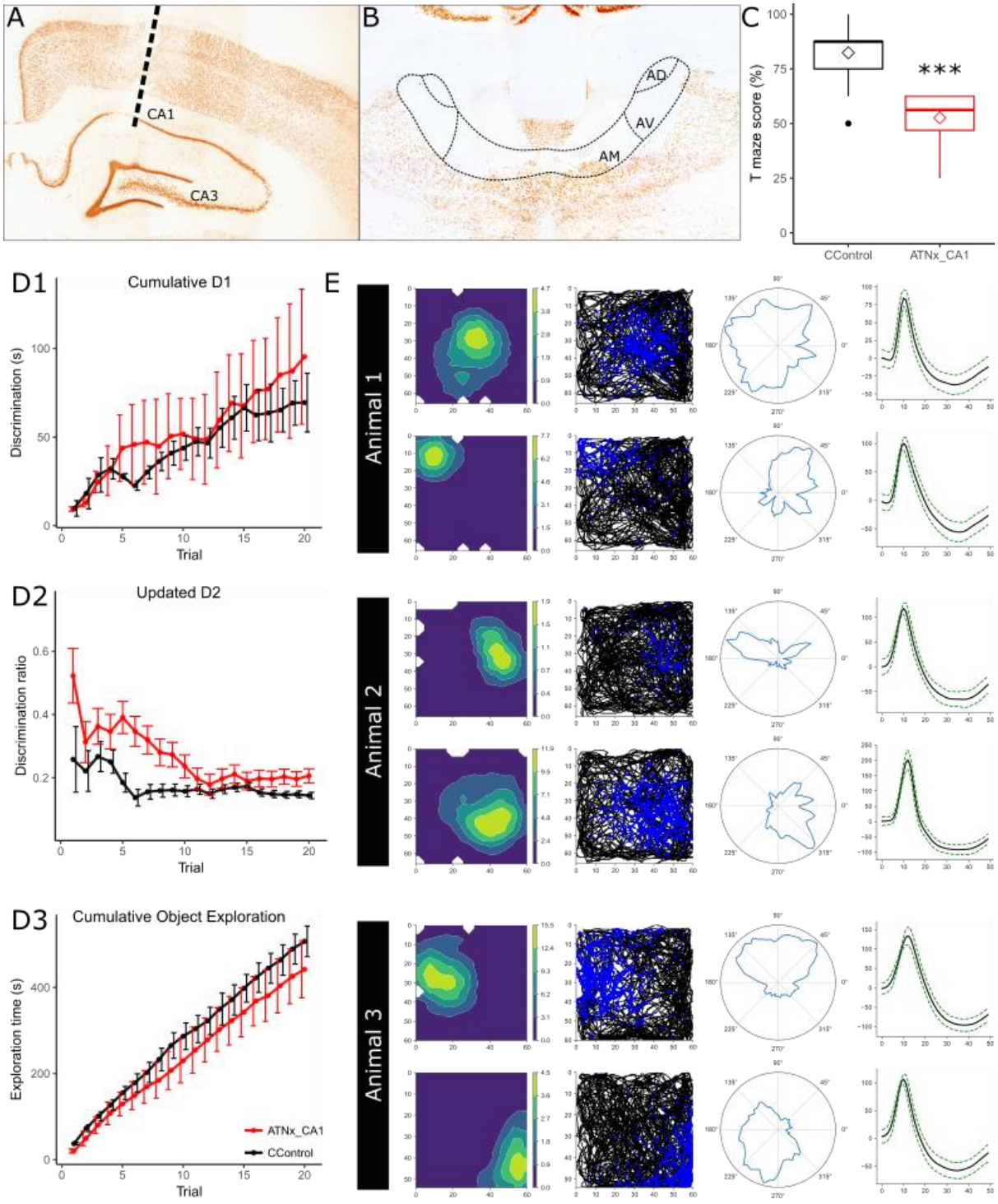

Fig 7: Representative electrode placement in CA1 (A) and ATN lesion (B), in NeuN-reacted sections. (C) Animals with ATN lesions and electrodes implanted in CA1 showed a signifcant deficit in spatial alternation task compared to controls animals (control data repeated from experiment 1). (D1-D3) The same cohort of ATNx animals showed no deficit in object recognition on bow tie maze. (E) Representative place cells recorded from CA1 in three ATNx animals.